Exp Astron (2016) 42:301–317
DOI 10.1007/s10686-016-9511-4

ORIGINAL ARTICLE

Experiments on the dish verification antenna china for the SKA

Xiaoming Chai[1,2] · **Bin Liu**[1,2] · **Lei Yu**[1] · **Shenghua Yu**[1] · **Di Wu**[1] · **Lijia Liu**[1]

Received: 20 April 2016 / Accepted: 19 September 2016 / Published online: 28 September 2016

Abstract The Square Kilometre Array (SKA) is expected to become the world's most powerful radio telescope at meter and centimeter wavelength in the coming decades. The construction of SKA will be divided into two phases. The first phase (SKA1), scheduled for completion in 2023, will construct 10 % of the whole collecting area. The second phase (SKA2) will build the rest 90 % collecting area. The SKA1 consists of several types of arrays including SKA1-low and SKA1-mid. The latter is a dish array consisting of ~200 medium-size antennas. The integrated dish array in SKA2 will expand to 2500 dishes, spreading 3000 kilometers across the southern part of Africa. The demanding specifications and enormous number of the SKA dish raise challenges in the dish development such as mass production with high performance at low cost, quick installation and high reliability. Dish Verification Antenna China (DVA-C) was built as one of three initial prototypes. A novel single-piece panel reflector made of carbon fiber reinforced polymer (CFRP) was adopted. In this study, an L-band receiver is installed to make DVA-C a complete system for experiments on antenna performance test and preliminary observations. The performance of DVA-C including the system noise temperature, pointing accuracy, antenna pattern, and aperture efficiency has been tested. Preliminary observations such as pulsars and HI are then conducted, which indicates that the DVA-C can not only serve as an educational instrument and key technology test bed, but also be applied for scientific work such as pulsar timing, all-sky HI survey, multi-frequency monitoring of variable sources etc.

✉ Bin Liu
bliu@nao.cas.cn

[1] Joint Laboratory for Radio Astronomy Technology, National Astronomical Observatories, Chinese Academy of Sciences, Beijing 100012, People's Republic of China

[2] Key Laboratory of Radio Astronomy, National Astronomical Observatories, Chinese Academy of Sciences, Nanjing 210008, People's Republic of China

Keywords Single-piece CFRP reflector · Pointing accuracy · Aperture efficiency · DVA-C · SKA

1 Introduction

The concept of Square Kilometre Array (SKA) [1] was proposed in the early 1990s by astronomers from more than ten countries. It will become the world's largest radio telescope and cover a wide frequency range from 50 MHz to at least 20 GHz, which makes it powerful enough to answer fundamental questions of science and laws of nature such as the origins of the universe [2]. The SKA will consist of three types of antenna arrays such as dish array (350 MHz to at least 20 GHz), low-frequency aperture array (50–350 MHz) and mid-frequency aperture array (400 MHz to1.7 GHz), extending across thousands of kilometers in the southern part of Africa and Australia. Nowadays around 100 research institutions and companies from all over the world are committing joint efforts on key technology development for SKA and detailed design for the first phase of SKA (SKA1). The construction of SKA1 is scheduled from 2018 to 2023. Significant discoveries on science are likely expected after 2020.

The SKA1 includes two types of antenna arrays such as SKA1-low and SKA1-mid [3] (see Fig. 1). The SKA1-low, part of the low-frequency aperture array, will consist of about 130000 log-periodic dual-polarized antenna elements. The SKA1-mid will be a mixed array of 133 15-m SKA dishes and 64 13.5-m MeerKAT dishes. In future the dish array will expand to about 2500 dishes, which are designed to achieve huge collecting area, high sensitivity, high survey speed and wide frequency coverage. These characteristics present enormous challenges in dish design and manufacture including mass production of thousands of dishes with identical performance, low cost, high reliability to reduce maintenance, ease of shipment, and quick installation. Thus, critical technologies should be developed i.e. exploring the possibility of using single-piece panel made of composite material such as carbon fiber reinforced polymer (CFRP) to replace traditional metal multi-panels for the medium-size antenna reflector [4].

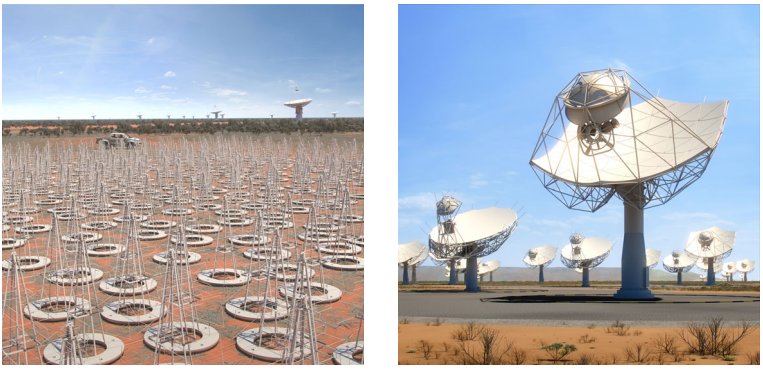

(a) SKA1-low (b) SKA1-mid

Fig. 1 Artists' impression of SKA1. The low-frequency aperture array (SKA1-low) is shown on the left, which consists of log-periodic antennas. The SKA1-mid is shown on the right, consisting of offset Gregorian dual-reflector dishes. (Source: the SKA official website, https://www.skatelescope.org)

China has participated in the concept design of the SKA dish since 2008. Two antenna concepts were presented to verify the antenna structure of the SKA dish by Joint Laboratory for Radio Astronomy Technology (JLRAT) from China in the SKA dish concept design review in 2011. One is an offset Gregorian dual-reflector antenna known as DVAC-1 and the other is a prime focus antenna known as DVAC-2 [5].

The SKA dish should be capable of accommodating five single pixel feeds, thus an offset structure such as DVAC-1 causes less blockage than the prime focus symmetric structure such as DVAC-2. Although the asymmetric offset structure increases the mechanical complexity, DVAC-1 has high aperture efficiency and low system noise temperature. The DVAC-2, on the other hand, has a symmetry structure that allows for simple optical and mechanical design while the blockage caused by feeds and their support truss lowers the aperture efficiency. The DVAC-1, now renamed as DVA-C, has been chosen as one of three options for SKA dish prototypes. The other two dish prototypes are DVA-1 [6] developed by the Canadian SKA Team and the MeerKAT type antenna [7] by the South African SKA team.

A unique single-piece panel reflector with skin-and-ribs structure is adopted by DVA-C to replace the traditional technique for large dimensional antennas which puts multiple panels together to form a complete reflector. This method can effectively reduce assembling time and manpower. The reflector is made of CFRP with surface metallization, because CFRP has high stiffness to weight ratio. The DVA-C was manufactured, integrated and ultimately built up in Aug. 2014 (Fig. 2). The main purpose of developing DVA-C is to validate the concept of single-piece panel reflector and to identify potential issues associated with the structure design or manufacturing process. Therefore not all the requirements of the SKA dish were considered in the design of DVA-C such as frequency range, cryogenic receivers, EMI/EMC issues etc. An L-band receiving system is first set up to make DVA-C a complete telescope to do several experiments. A pointing model is developed to correct mechanical misalignments and static and dynamic flexure in the structure and software compensation is performed to improve the pointing accuracy. The performance of DVA-C, including system noise temperature, antenna pattern, and aperture efficiency are then measured. Preliminary observations of pulsars and HI in the Galaxy have been conducted.

Fig. 2 Photograph of the DVA-C prototype. The DVA-C is an offset Gregorian dual-reflector antenna, and the feed is located at the secondary focus. "Feed-up" configuration is adopted, in that the sub-reflector and the feed are above the main reflector while pointing to the horizon

Moreover, potential scientific study by DVA-C and its collaboration with Five-hundred-meter Aperture Spherical radio Telescope (FAST) [8] are discussed.

2 General specification of DVA-C and test system description

2.1 Technical specification of DVA-C

The offset Gregorian dual-reflector antenna with feed-down configuration is finally selected by SKA. The performance requirements of the SKA dish were updated after the SKA1 re-baseline design [3] (see Table 1). The main technical specifications of DVA-C are listed in Table 2. It is an offset Gregorian dual-reflector antenna with feed-up configuration to reduce noise from spillover, and shaped optical design is made to further improve the aperture efficiency.

The optical design, structure design and servo system of DVA-C is introduced in the paper [9]. DVA-C adopts a novel approach for the reflectors. Traditionally panels made of aluminum are assembled together to make the main reflector which dimensions are 18 m × 15 m. Considering special requirements of the SKA dish including mass production, fast installation, low cost and minimal manpower, a single-piece panel reflector made of composite material is examined. The panel of the reflector adopts skin-and-ribs structure as shown in Fig. 3. The size of the main reflector makes it one of

Table 1 Performance requirements of the SKA dish

Equivalent aperture diameter	15 m
Frequency range	350 MHz–20 GHz
Optics	Clear aperture
Aperture efficiency[a]	~60 % (350 MHz), ~ 65 % (400 MHz), ~ 78 % (0.6–8 GHz), ~ 70 % (8–15 GHz), ~ 65 % (15–20 GHz)
Total spillover noise	3 K (L-band)
Other losses	<2 K (L-band)
First sidelobe	−21 dB
Far-out sidelobe level	< −50 dB
Receivers[b]	Cryo-cooled; Band 1: 0.35–1.05 GHz; Band 2: 0.95–1.76 GHz; Band 3: 1.65–3.05 GHz; Band 4: 2.8–5.18 GHz; Band 5: 4.6–13.8 GHz;
Elevation limit	<15°
Azimuth range	±270 °
Pointing accuracy:	<10″ (Precision); < 17″ (Standard); <180″ (Degraded)
Classes of environmental operating conditions	Precision: wind <7 m/s; night Standard: wind <7 m/s; day Degraded: wind <20 m/s

[a] Expected aperture efficiency using well designed and realizable feeds

[b] Three of the five receivers will be developed in SKA1 in priorities of band 2, 5 and 1. The other two are scheduled in SKA2

Table 2 Main technical specifications of DVA-C

Antenna type	Offset Gregorian dual reflectors, feed-up
Optics	Shaped
Equivalent aperture diameter	15 m
Mount type	Elevation-and-azimuth mount
Reflector structure	CFRP single piece panel reflectors with skin-and-ribs structure
Reflector surface accuracy	<0.8 mm
Frequency	350 MHz–10 GHz
Focal ratio of main reflector (f/D)	0.36
Illumination angle	55°
Aperture efficiency	~70 % (L-band)
First sidelobe	< −21 dB
Far-out sidelobe	< −50 dB
Feed indexer	Accommodating 3 feeds, feed switching time < 30 s
Elevation range	15°–95°
Azimuth range	±270 °

the world's largest panels using CFRP, which represents a huge challenge for fabrication. The skin is a 2-mm thick layer of carbon fiber with surface metallization. It was manufactured by vacuum injection molding process (VIMP). First the mold for the skin was prepared and its surface was metallized. Then fiber fabrics were laid out on the mold and infusion runners were also spread out. After resin was injected, carbon fibers

Fig. 3 Main reflector of the DVA-C with its backup structure. The main reflector is a single-piece panel with skin-and-ribs structure and it is made of CFRP. And the backup structure is made of steel (the white truss part in the photograph)

and the resin were polymerized together by vacuum process. The ribs were also manufactured by the VIMP and employ a sandwich structure of fiber fabrics and foam to increase the reflector stiffness. After the skin and ribs were prepared well separately, they were bonded by adhesive. Then the panel was released from the mold and further repair and inspection work needed to be done before the main reflector was completed. The surface accuracy has been measured by photogrammetry and root mean square (RMS) of the accuracy reaches 0.8 mm. The sub-reflector with a dimension of 5.0 m × 4.7 m also adopts CFRP single piece panel. The backup of the reflectors are made of steel.

2.2 Test system description

The feeds and low noise amplifiers (LNAs) of the SKA dish are still under development by the SKA Dish Consortium. As a preliminary attempt, an ambient temperature L-band receiver is utilized to demonstrate the performance of DVA-C and to conduct experimental astronomical observations. A linearly polarized corrugated horn at L-band is used and its ohmic loss is about 0.2 dB. It is necessary to note that the receiving system only records the signal of a single linear polarization.

The schematic of the entire test system is shown in Fig. 4. The working flow is presented as follows: firstly, through a very short high-quality coaxial radio-frequency (RF) line, the feed is connected to an LNA; secondly, a tunable band-pass filter is applied to define the required bandwidth and minimize the radio frequency interferences (RFIs); thirdly, another LNA is installed to increase the gain of the system, meanwhile reduce the noise contribution of the following components that will be described later. These devices mentioned above are situated on the feed indexer. Then

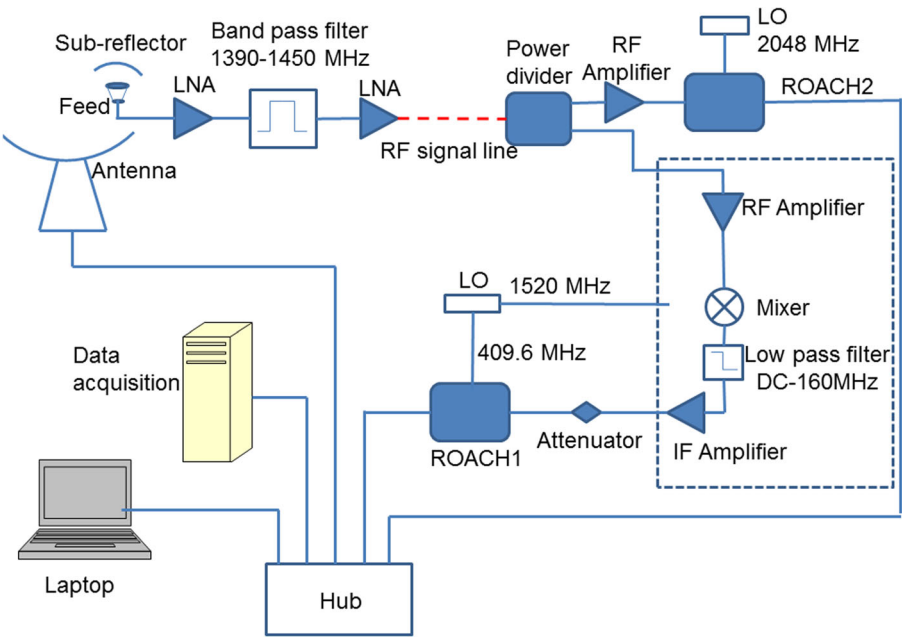

Fig. 4 Block diagram of the test system for DVA-C

through a 30-m-long RF signal line, signals are transmitted to a power divider placed in the shielded compartment of the pedestal. The power divider distributes the RF signal among two outputs. The idea here to divide the signal is to improve the observing efficiency and to compare the outputs of RF signal with ROACH2 and IF signal with ROACH1.

Path 1 is via a RF amplifier and then leads to ROACH2, which is used for pulsar observation. Path 2 is via a RF amplifier, a mixer, a low-pass filter, an intermediate-frequency (IF) amplifier and an attenuator to convert the RF signal to IF signal. At last the IF signal is transmitted to ROACH1, which is used for antenna performance test such as pointing and aperture efficiency. The total gain from the antenna to ROACH1 is about 80 dB. The devices in the two paths are placed in the compartment of the pedestal. The detailed key characteristics of the two signal paths are listed in Table 3.

3 Performance test

3.1 Antenna noise temperature of DVA-C

The system noise temperature of a radio telescope (T_{Sys}) includes three parts: the equivalent noise temperature of the antenna (T_{Ant}), the equivalent noise temperature of passive loss of feed, waveguide and polarizer (T_{Feed}), and the equivalent noise temperature of the receiver (T_{Rec}). T_{Ant} represents noise from the sky (cosmic microwave background, atmosphere loss, etc.), ground radiation, spillover, and any ohmic losses of the antenna. T_{Ant} of the DVA-C is simulated and analyzed by electromagnetic modeling of the antenna and feed. The results are shown in Fig. 5. It can be seen that T_{Ant} at L-band is about 10 K.

In this study, the system noise temperature of DVA-C (T_{Sys}) is tested by Y-factor method and the noise temperatures of the receiver (T_{Rec}) and feed (T_{Feed}) are measured in the lab, then the actual antenna noise temperature can be deduced.

The antenna first points to cold sky (away from the Galactic Plane and other strong radio sources) and the noise power received is recorded as P_{OFF}. Then a matched load at room temperature, replacing the feed, is connected to the front-end of the receiver and the noise power P_{Load} is recorded. The Y-factor is defined as

$$Y = \frac{P_{Load}}{P_{OFF}} = \frac{T_{Load} + T_{Rec}}{T_{Sys}} = 3.4. \quad (1)$$

T_{Rec} is measured by the Noise Figure Analyzer (Agilent N8974A) in the lab and it is about 80 K. And T_{Load} is taken to be 300 K. From Eq. (1) T_{Sys} can be obtained as 110 K.

Table 3 Key characteristics of the two signal paths

Path	Centre frequency	Bandwidth	Sample frequency	Channel bandwidths	Sample bits
1	1420 MHz	60 MHz	2 GHz	1 MHz	8 bits
2	100 MHz	60 MHz	409.6 MHz	204.8 KHz	8 bits

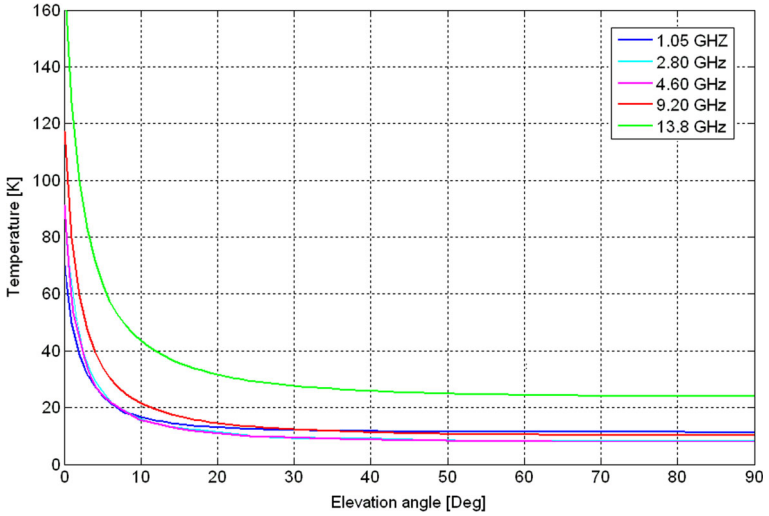

Fig. 5 Simulation results of the antenna noise temperature of DVA-C. It is analyzed along with variation of elevation angles at different frequencies from 1.05 to 13.8 GHz. Noise contributions from ground, atmosphere and sky are included

Since the ohmic loss of the feed and orthogonal mode transducer is about 0.2 dB and the physical temperature of the feed T_0 is about 300 K, this would result in a T_{Feed} of about 14 K.

From the measured T_{Sys}, T_{Rec} and T_{Feed}, the antenna noise temperature $T_{Ant} = 16$ K is derived. This result agrees well with the simulation (Fig. 5).

3.2 Antenna pointing calibration

Pointing accuracy is a significant indicator of the performance of a radio telescope. Due to atmospheric refraction, manufacturing and assembling errors, structural deformations caused by gravity, wind and temperature, etc., the telescope cannot point exactly toward a radio source without a calibration. In this section, the pointing error of DVA-C is first analyzed. Then a first-order pointing model is applied to meet the pointing requirement.

3.2.1 Antenna pointing error analysis

The antenna pointing error can be decomposed into an azimuth and elevation component. These deviations are caused by the collimation error that the elevation axis is not exactly perpendicular to the beam axis, the azimuth-axis tilt error, the azimuth- and elevation-axes coding zero-errors, gravitational deflection error, and atmospheric refraction error and so on. The antenna pointing of DVA-C is determined by the center of the −3 dB beam contour. Pointing deviation is the difference between the ideal pointing position and the actual position. The RMS of the pointing deviation in the azimuth of the antenna δ_A can be expressed as

$$\delta_A = \sqrt{\frac{\sum_{i=1}^{n} [\delta_{Ai} \times \cos(E_i)]^2}{n}}, \tag{2}$$

where δ_{A_i} is the pointing error in the azimuth of the i-th pointing, and E_i is the elevation angle each time. And the RMS of the pointing deviation in the elevation of the antenna δ_E is:

$$\delta_E = \sqrt{\frac{\sum_{i=1}^{n} [\delta_{E_i}]^2}{n}}, \tag{3}$$

where δ_{E_i} is the pointing error in the elevation of the i-th pointing.

Then the total RMS pointing error δ is

$$\delta = \sqrt{{\delta_A}^2 + {\delta_E}^2}. \tag{4}$$

In this study, the following radio sources are chosen to calibrate the antenna pointing: Cygnus A (Cyg A), Cassiopeia A (Cas A), Taurus A (Tau A), Orion A (Ori A), Virgo A (Vir A), 3C286, and 3C295. Along with variations of their position, the pointing data acquired are evenly distributed on the celestial sphere and cover a large area, as shown in Fig. 6.

With the Eqs. (2) and (3), the initial deviations in the azimuth and elevation before the calibration is calculated, and they are 19.8′ RMS and 6.5′ RMS separately. The total pointing error is 20.8′ RMS by Eq. (4).

In the next section, the pointing model will be established and the error will be corrected to improve the pointing accuracy.

3.2.2 First-order pointing model

Table 4 shows detailed error sources that cause the pointing error of the antenna. The pointing error in the azimuth or in the elevation can be regarded as an algebraic

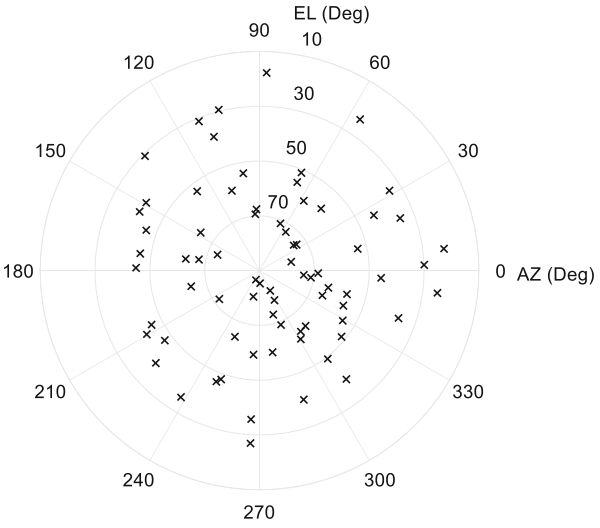

Fig. 6 The sky coverage of the sources used for pointing calibration

Table 4 Pointing error sources of a radio-telescope antenna

Symbols	Error sources
C_a	Azimuth coding zero-error
C_e	Elevation coding zero-error
S_a	Azimuth encoder error
S_e	Elevation encoder error
γ	Electric axis without calibration
η	Non-orthogonal elevation axis and azimuth axis
Ψ_x	Azimuth axis tilting error to north
Ψ_y	Azimuth axis tilting error to east
ξ_{B1}	Azimuth bearing offset to north
ξ_{B2}	Azimuth bearing offset to east
ξ_{B3}	Elevation bearing offset to north
ξ_{B4}	Elevation bearing offset to east
δ	Structural deformation by gravity
λ	Atmospheric refraction

combination of these sources in a first-order pointing model, because these error components are relatively small.

Then the linear pointing models [10] can be expressed as

$$\begin{aligned}\delta_{A_i} = C_a + S_a A_i + \gamma \sec E_i - \eta \tan E_i - \Psi_x \sin A_i \tan E_i - \Psi_y \cos A_i \tan E_i + \xi_{B1} \sin E_i + \\ \xi_{B2} \cos E_i - \quad \xi_{B3} \cos A_i \sin A_i \tan E_i - \quad \xi_{B4} \cos A_i \cos A_i \tan E_i + \quad \varepsilon_{A_i},\end{aligned} \tag{5}$$

and

$$\begin{aligned}\delta_{E_i} = C_e + S_e E_i - \Psi_x \cos A_i + \Psi_y \sin A_i - \xi_{B3} \cos A_i \cos A_i + \xi_{B4} \cos A_i \sin A_i + \delta \cos E_i + \\ \lambda \qquad\qquad \cot E_i + \qquad\qquad \varepsilon_{E_i},\end{aligned} \tag{6}$$

where A_i is the azimuth angle and E_i is the elevation angle, ε_{A_i} and ε_{E_i} are random factors in the solving process of the model.

The Cross-Scan observing mode was taken for the pointing measurements. The measurements were conducted during both the day and night and the general environmental conditions were standard. The DVA-C locates in an antenna manufacturing factory in Shijiazhuang, and suffers from much RFI, which increases difficulties in data processes of the pointing model. In this study, a data processing method of RANSAC [11] is explored. Parameters of the pointing model are obtained and given in Table 5.

3.2.3 Results of pointing calibration

With the pointing model, errors in the azimuth and elevation after calibration are obtained. Comparing them with the initial pointing errors, the residual error or pointing accuracy is acquired and shown in Fig. 7.

Table 5 The values of parameters in the pointing model

Parameter	Value (°)	Parameter	Value (°)
C_a	1.6015	Ψ_y	−0.0191
C_e	0.0000	ξ_{B1}	−1.9653
S_a	−0.0002	ξ_{B2}	−2.2183
S_e	−0.0314	ξ_{B3}	−0.0383
γ	−2.2995	ξ_{B4}	−0.0006
η	1.1378	δ	−1.7021
Ψ_x	−0.0200	λ	−0.4245

The accuracy in the azimuth improves from 19.8′ to 2.2′ RMS, whilst the accuracy in the elevation improves from 6.5′ to 4.2′ RMS. The total pointing accuracy of 4.7′

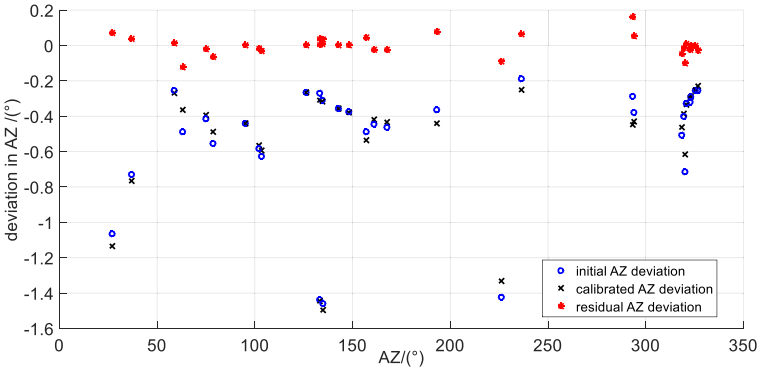

(a) Deviations in the azimuth before and after calibration. The blue circles show pointing deviations in the azimuth before calibration. The black ‘x’ symbols show the calibrated deviations in the azimuth by the pointing model. The red ‘*” symbols show the residual deviations in the azimuth.

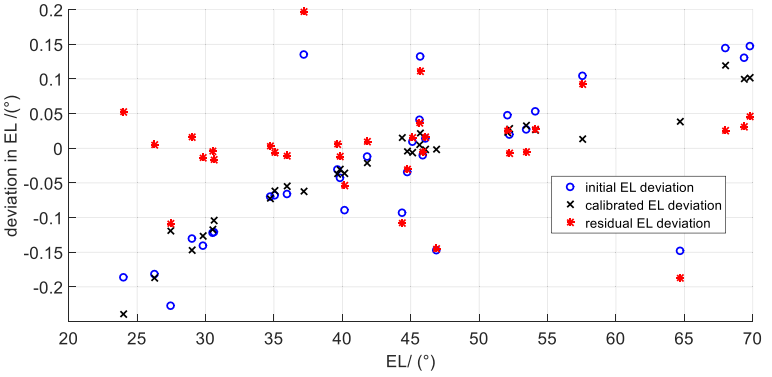

(b) Deviations in the elevation before and after calibration. The blue circles show pointing deviations in the elevation before calibration. The black ‘x’ symbols show the calibrated deviations in the elevation by the pointing model. The red ‘*” symbols show the residual deviations in the elevation.

Fig. 7 Results of pointing calibration

RMS can be obtained after calibration. By combining the observational error of the raw data and the pointing model fitting error, the final estimated measurement error is given as ~0.1′. The result of pointing calibration shown here is limited by some factors such as the operating frequency of the test receiver, quality of data used in the pointing model etc.

For single dish radio telescopes, less than 10 % of the antenna's half-power beam width is generally acceptable for antenna pointing deviation, thus the current pointing accuracy of DVA-C can meet this requirement at L-band working in the single dish mode.

It is worth noting that the working frequency of SKA dish antenna is up to 20 GHz. This requires that the pointing accuracy is much higher than the present accuracy. Efforts for further pointing improvement such as precisely mechanical adjustment and accurately pointing modeling should be taken in future.

3.3 Antenna pattern

An L-band geostationary satellite AsiaStar is observed to measure the far-field antenna pattern of DVA-C. The longitude of AsiaStar is 105° east and its spectrum covers the frequency range 1452–1492 MHz. The signal of AsiaStar is of circular polarization. Cross-scan method is adopted to acquire the antenna pattern both in the azimuth and elevation directions. Figure 8 shows the antenna pattern when the antenna made scans in the azimuth. The half-power beamwidth is about 0.95°. The first sidelobe is lower than −23 dB which meets the requirement for first sidelobe. The difference between two first sidelobes is about 2 dB. The measurements of beamwidth and first sidelobe level match up with the simulated radiation pattern (seen in [9] and also described in Fig. 8).

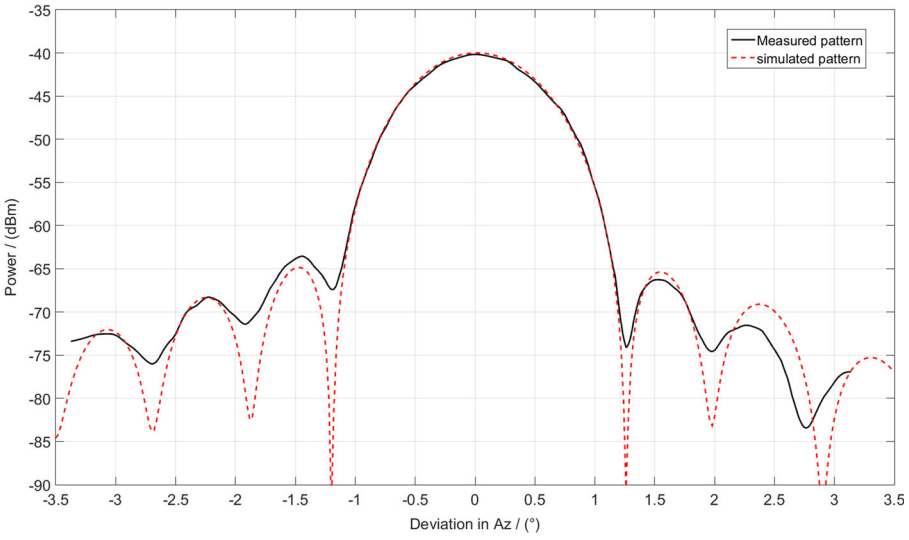

Fig. 8 Far-field pattern of DVA-C. The solid line shows the measured antenna pattern. The dashed line represents the simulated pattern [9]. The measured main beam matches well with the simulated result. The first sidelobe is less than −23 dB which meets the SKA performance requirements for antenna

3.4 Aperture efficiency

Aperture efficiency of DVA-C can be measured by observing proper radio sources. For DVA-C, Cyg A, Cas A and Tau A are chosen. At L-band the flux densities of these sources [12, 13] are: 1800±50 Jy (Cas A), 1660±50 Jy (Cyg A) and 940±10 Jy (Tau A).

The aperture efficiency can be calculated with the following equation:

$$\eta = \frac{2kT_{SYS}(Y-1)}{S_V A_g}. \tag{7}$$

Here, η is the aperture efficiency, k is Boltzmann's constant, T_{Sys} is the system noise temperature, S_V is the flux density of the radio source, A_g is the physical aperture of the antenna, and Y is a factor expressed as following

$$Y = \frac{P_{\mathrm{ON}}}{P_{OFF}}. \tag{8}$$

P_{ON} is the power received when the antenna is pointing to a radio source while P_{OFF} is the power received when the antenna is pointing to cold sky. These power values are collected by ROACH1.

DVA-C tracks three sources separately as they rise up and down to acquire the variation of aperture efficiency along with the change of elevation angles. The results are shown in Fig. 9.

The average aperture efficiency is slightly different when using different radio sources to measure. That is 76 % by CasA, 73 % by CygA and 68 % by TauA. These differences can be attributed by the flux uncertainties of difference sources.

Three factors contribute to the total measurement error, which are Y, S_V and T_{Sys}. Their effects on the aperture efficiency are listed in Table 6. On the basis of the error transfer principle, we can get the total measurement errors: 9.9 % by Cas A, 9.6 % by Cyg A and 7.6 % by Tau A.

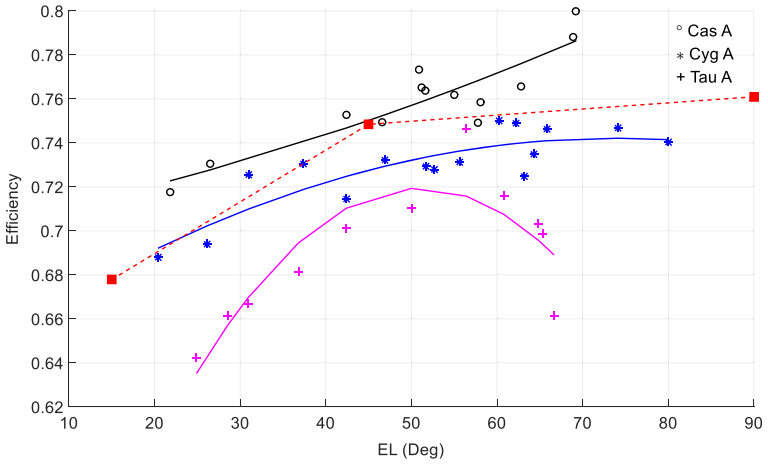

Fig. 9 Aperture efficiency varying with elevation. The red square symbol shows the simulation result from structural analysis and electromagnetic modeling. Other symbols and lines show the test results

Table 6 Measurement error analysis of aperture efficiency

Measurement error sources	Cas A $\Delta\eta$ (%)	Cyg A $\Delta\eta$ (%)	Tau A $\Delta\eta$ (%)
ΔY	0.9	0.8	0.7
ΔS_V	2.1	2.2	0.7
ΔT_{Sys}	6.9	6.6	6.2
Total	9.9	9.6	7.6

This is an attempt to measure the gain of the DVA-C. Though a simple ambient temperature single polarization receiver is used, the results do give an indication of the aperture efficiency. Parallactic angle effect is clear seen when observing Tau A due to the intrinsic polarization property of the source.

A rough estimation of the aperture efficiency of the DVA-C, using the L-band Feed current being used, has been simulated. Data on the gravitational deformation of the antenna obtained by the structural analyses has been used to calculate the gain along with elevation angles. At 1.4 GHz, the simulated aperture efficiencies are 67.79 % at the elevation angle of 15°, 74.85 % at the elevation angle of 45°, and 76.1 % at the elevation angle of 90°.

4 Experimental observations and possible future science

Equipped with the L-band receiver, the DVA-C prototype is used as a single dish radio telescope to demonstrate radio astronomical observations, such as monitor strong radio sources including pulsars and HI mapping of the Milky Way.

As mentioned in Section 3, the flux measurements are performed to test the system performance including the pointing and aperture efficiency. The cross-scan observing mode is applied. A control software is developed for this mode enabling the astronomical observations. Since its protocol is designed for multiple dish elements, our software may also act as a pathfinder for the SKA dish array.

Figure 10 shows the result of observation of pulsar B0329+54, which is one of the strongest pulsars at L-band in the northern sky. After the RFI excision, dispersion removal, and folding with the PSRSOFT tools, and with integration time of 20 min and bandwidth of 50 MHz, clear pulse profile could be seen with a signal to noise ratio of about 62. Similarly, another two pulsars B1933+16 and B2020+28 are observed by DVA-C with clear profiles. Moreover, the HI spectra were also observed and shown in Fig. 11.

These preliminary observations illustrate that, in addition to serve as an experimental platform or an educational tool, this telescope may also have the potential to produce scientific outcomes. Cryogenically cooled receiver could be utilized to optimize the sensitivity. Moreover, C- and Ku-band receivers have been designed and manufactured, which may enable high frequency observations with DVA-C. Pulsar timing, all-sky HI survey, multi-frequency monitoring of variable sources and IPS observations may be among the possible scientific observations using DVA-C.

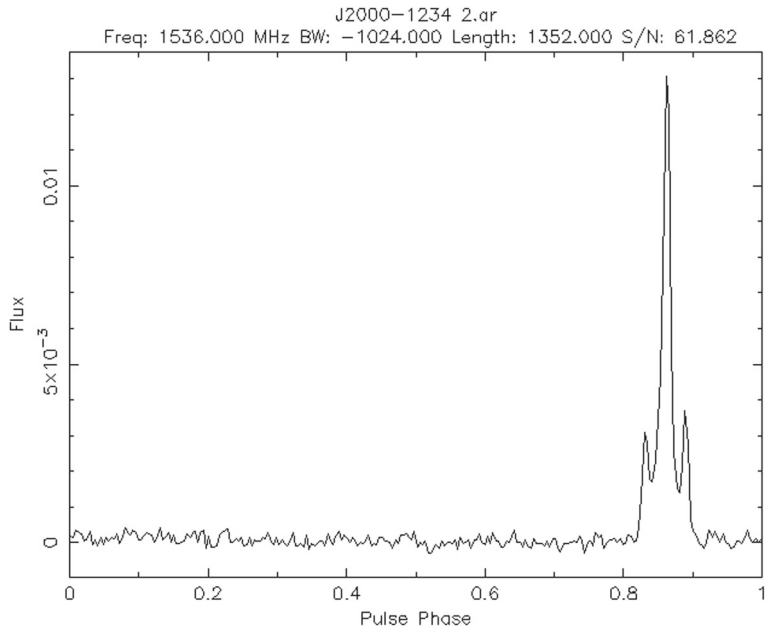

Fig. 10 Observation on pulsar B0329+54

The construction of FAST will be completed in Sep. 2016. DVA-C is currently playing some roles in technique verification and observation software preparation for the FAST operation. For example, the 19 elements phased array feed (PAF) at L-band for FAST will be first installed on DVA-C to test its performance [14]. With the PAF, the DVA-C can monitor a certain number of pulsars to form a Pulsar Timing Array. The technique and software will be also applicable for the pulsar timing project of FAST.

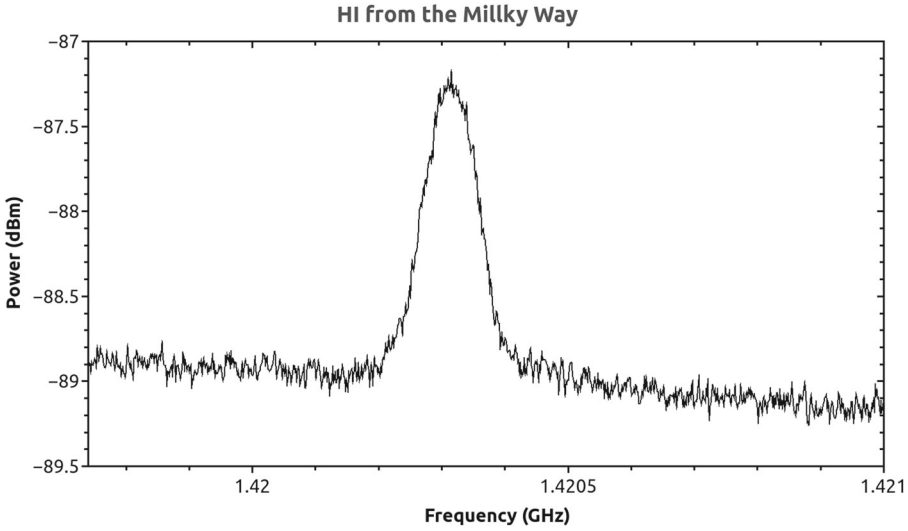

Fig. 11 Observation on HI from the galaxy. The spectrum is measured toward the Galactic Plane (187.0, +0.0) [9]

Besides, DVA-C can be re-located near the site of FAST. The DVA-C will then be helpful for foreground extinction of cosmic HI observations by FAST. Some work for FAST will be better conducted by the collaboration with DVA-C, such as RFI mitigation and holographic measurement of the main reflector of FAST.

5 Conclusion

The DVA-C is a prototype to verify key technology development for the SKA dish. An L-band receiver is assembled to the antenna of DVA-C to make it a complete telescope. The testing results demonstrate that the capability of DVA-C has already met the expected requirements at L-band. Experimental observations are also conducted. Conclusions can be drawn as follows:

(1) The pointing accuracy after calibration can reach 4.7′ RMS, meeting the requirement at L-band. However, further efforts should be made to meet the demanding specification of SKA1-mid at higher frequencies.
(2) Measurements of the aperture efficiency agree with predictions from structural analysis. It is about 70 % at L-band which is sufficient for experiments and preliminary observations.
(3) The performance results i.e. antenna noise temperature and aperture efficiency also indicate that the single-piece panel CFRP reflector of large scale is a potential choice for radio-telescope antenna besides the traditional aluminum panel.
(4) The DVA-C is a good educational instrument and key technology test bed such as technique and software preparation for FAST. It also can be applied to experimental observations and maybe limited scientific observations in future.

Now the second prototype of DVA-C, namely SKA-P (SKA Prototype), is under design, which is the ultimate prototype for the SKA dish. Experience from the work in this paper including performance test and experimental observations will be valuable for SKA-P.

Acknowledgments The authors acknowledge the assistance of Biao Du, Yuanpeng Zheng, Yang Wu, Xuguang Geng, and Long Chen at the 54th Research Institute of the China Electronics Technology Group Corporation during the test process. Again, the authors acknowledge Bo Peng, Chengjin Jin and Jianbin Li at National Astronomical Observatories, Chinese Academy of Sciences for discussions on this study. This work is sponsored by the Chinese Ministry of Science and Technology under the State Key Development Program for Basic Research (No. 2013CB837900 and No. 2012CB821800), and National Natural Science Foundation of China (No.11261140641, No. 11303057 and No. 11503036).

References

1. Taylor, A.R.: The square kilometre array. Proc. Int. Astron. Union **8**(S291), 337–341 (2012)
2. Carilli, C., Rawlings, S.: Science with the square kilometer array: motivation, key science projects, standards and assumptions. arXiv preprint astro-ph/0409274 (2004)
3. Dewdney, P.: SKA1 system baseline V2 description, SKA document SKA-TEL-SKO-0000308 (2015)

4. Dewdney, P.E., Hall, P.J., Schilizzi, R.T., Lazio, T.J.L.: The square kilometre array. Proc. IEEE **97**(8), 1482–1496 (2009)
5. Chai, X., Du, B., Zheng, Y., et al.: Dish Verification Antenna China for SKA. In Antennas & Propagation (ISAP), 2013 Proceedings of the International Symposium on IEEE. Vol. 1, pp. 33–36 (2013)
6. Lacy, G.E., Fleming, M., et al.: An update on the mechanical and EM performance of the composite dish verification antenna (DVA-1) for the SKA. In Electromagnetics in Advanced Applications (ICEAA), 2012 International Conference on. IEEE. pp. 388–391 (2012)
7. Davidson, D.B.: MeerKAT and SKA phase 1. In Antennas, Propagation & EM Theory (ISAPE), 2012 10th International Symposium on. IEEE. pp. 1279–1282 (2012)
8. Nan, R., Li, D., Jin, C., et al.: The five-hundred-meter aperture spherical radio telescope (FAST) project. Int. J. Mod. Phys. D **20**(06), 989–1024 (2011)
9. Du, B., Zheng, Y., Wu, Y., et al.: DVA-C: a Chinese Dish Prototype for the Square Kilometre Array. International Symposium of Antenna and Propagation, Tasmania, Australia, Nov 9–12, pp. 908–911 (2015)
10. Zhao Y.: Research on modeling analysis and design of pointing errors for large radio telescope, Xidian University, Phd thesis (2008)
11. Fischler, M.A., Bolles, R.C.: Random sample consensus: a paradigm for model fitting with applications to image analysis and automated cartography. Commun. ACM **24**(6), 381–395 (1981)
12. Onic D., Urosevic D.: On the continuum radio spectrum of CAS A: possible evidence of nonlinear particle acceleration. Astrophys. J. **805**:119 (6 pp) (2015)
13. Baars, J.W.M., Genzel, R., Pauliny-Toth, I.I.K., Witzel, A.: The absolute spectrum of Cas A; An accurate flux density scale and a set of secondary calibrators. Astron. Astrophys. **61**, 99–106 (1977)
14. Wu, Y., Du, B., et al.: Optical design of the China Dish verification antenna for the Square Kilometre array. In General Assembly and Scientific Symposium (URSI GASS), 2014 XXXIth URSI (pp. 1–4). IEEE (2014)